entropy

MDPI

Article

Quantum Work Statistics with Initial Coherence

María García Díaz [1], Giacomo Guarnieri [2] and Mauro Paternostro [3,*]

1 Física Teòrica: Informació i Fenòmens Quàntics, Departament de Física, Universitat Autònoma de Barcelona, ES-08193 Bellaterra (Barcelona), Spain; maria.garciadia@e-campus.uab.cat
2 School of Physics, Trinity College Dublin, College Green, Dublin 2, Ireland; guarnieg@tcd.ie
3 Centre for Theoretical Atomic, Molecular, and Optical Physics, School of Mathematics and Physics, Queen's University, Belfast BT7 1NN, UK
* Correspondence: m.paternostro@qub.ac.uk

Received: 23 September 2020; Accepted: 22 October 2020; Published: 27 October 2020

Abstract: The two-point measurement scheme for computing the thermodynamic work performed on a system requires it to be initially in equilibrium. The Margenau–Hill scheme, among others, extends the previous approach to allow for a non-equilibrium initial state. We establish a quantitative comparison between both schemes in terms of the amount of coherence present in the initial state of the system, as quantified by the l_1-coherence measure. We show that the difference between the two first moments of work, the variances of work, and the average entropy production obtained in both schemes can be cast in terms of such initial coherence. Moreover, we prove that the average entropy production can take negative values in the Margenau–Hill framework.

Keywords: quantum coherence; quantum thermodynamics; work distribution

1. Introduction

In the quest for the understanding of the interplay between thermal and quantum fluctuations that determine the energy exchange processes occurring at the nano- and micro-scale, the identification of the role played by quantum coherences is paramount [1,2]. The foundational nature of such understanding has been the driving force for much research effort, which has started shedding light onto the role that quantum coherence has in the quantum thermodynamic phenomenology, from work extraction to the emergence of irreversibility [3–12]. Owing to the success that it has encountered in classical stochastic thermodynamics, the current approach to the determination of the statistics of such energetics in the quantum domain is based on the so-called two-point measurement (TPM) protocol [13–15]: the energy change of a system driven by a time-dependent protocol is measured both at the initial and final time of the dynamics. The application of the TPM protocol has led to the possibility to address the statistics of quantum energy fluctuations in a few interesting experiments [16–20]. Unfortunately, such a strategy has a considerable drawback in that, by performing a strong initial projective measurement, all quantum coherences in the energy eigenbasis are removed, de facto washing out the possibility of quantum interference to take place.

This fundamental bottleneck has led to efforts aimed at formulating coherence-preserving protocols for the quantification of the statistics of energy fluctuations resulting from a quantum process [21–24]. A particularly tantalising one entails the use of quasi-probability functions to account for such statistics [21,25–27]. Drawing from the success that quasi-probability distributions have in signalling non-classical effects in the statistics of light fields, the authors of [21,23] have put forward the cases for the Margenau–Hill (MH) quasi-probability distribution [28,29] for the energetics of a quantum process. The MH distribution, which is the real part of the well-known complex Kirkwood distribution [30], provides the probability distribution for any two non-commuting observables and can take negative values. In the context of stochastic thermodynamics, the distribution of energy

fluctuations provided by the MH approach generalises the TPM one by replacing the strong initial measurement requested by the latter with a weak measurement.

Negative values of the statistics inferred following the ensuing protocol witness strong non-classicality of the overall process followed by the system [23], which are completely removed from the picture provided by TPM. In such a context, it is crucial to pinpoint the role that the quantum coherences either present in the initial state of the system or created throughout its dynamics have in the setting up of the MH phenomenology. This is precisely the point addressed in this paper, where we thoroughly investigate the differences between the statistics entailed by the TPM and MH approaches and relate them to the value taken by well-established quantifiers of quantum coherence [31] over the initial state of the system, as well as dynamical features of the process that the latter undergoes. We show that such coherence-depending differences have strong implications for the formulation of statements on the degree of irreversibility of a non-equilibrium process provided by the MH approach, and provide a re-formulation of the average entropy production that clearly highlights the contribution resulting from quantum coherences. This work thus makes the first necessary steps towards the quantitative understanding of the implications of quantum coherence for the phenomenology of the statistics of energy fluctuations in the quantum domain.

The remainder of this paper is organised as follows: In Section 2.1, we present a detailed description of the TPM and MH schemes. Section 2.2 is a brief introduction to coherence theory. The distance between the first moments of work obtained in both schemes is related to initial coherence throughout Section 3.1. A similar investigation is carried out for the variances of work and the average entropy production, which can be found in Sections 3.2 and 3.3, respectively. In Section 4, we draw our conclusions, while we defer a series of technical details, including the demonstration of the main results of our work, to the accompanying Appendix.

2. Background

2.1. Quantum Work Statistics

Consider an isolated quantum system initially prepared in an equilibrium state and subjected to an external force that changes a work parameter λ_t in time according to a generic finite-time protocol. The latter includes, at the initial time $t = 0$ and final time $t = \tau$, projective measurements of the energy of the system, which result in the values $E_n^{\lambda_0} \equiv E_n^0$ and $E_m^{\lambda_\tau} \equiv E_m^\tau$. Here, n and m label the respective energy levels of the initial and final Hamiltonian $H(\lambda_0) \equiv H_0$, $H(\lambda_\tau) \equiv H_\tau$ of the system. Thermal and quantum randomness render the measured energy difference $E_m^\tau - E_n^0$, which can be interpreted as the work done on the system through the protocol, a stochastic variable. One can recognize here the well-known two-point measurement (TPM) scheme for measuring work, whose values are distributed according to the following probability distribution:

$$p_\tau^{\mathrm{TPM}}(w) = \sum_{m,n} P_\tau^{\mathrm{TPM}}[E_m^\tau, E_n^0]\delta[w - (E_m^\tau - E_n^0)]. \tag{1}$$

Here, $P_\tau^{\mathrm{TPM}}[E_m^\tau, E_n^0]$ is the joint probability to measure the energy values E_n^0 and E_m^τ,

$$P_\tau^{\mathrm{TPM}}[E_m^\tau, E_n^0] = \mathrm{Tr}\left[\Pi_{E_m^\tau} U_\tau \Pi_{E_n^0} \mathcal{G}_0 \Pi_{E_n^0} U_\tau^\dagger \Pi_{E_m^\tau}\right], \tag{2}$$

where $\mathcal{G}(\lambda_t) \equiv \mathcal{G}_t = e^{-\beta H_t}/Z_t$ is a Gibbs state—at the inverse temperature β—of the instantaneous Hamiltonian $H(\lambda_t) \equiv H_t = \sum_i E_i^t \Pi_i^t$, $Z_t = \mathrm{Tr}\left[e^{-\beta H_t}\right]$ is the associated partition function, $\Pi_i^t = |E_i^t\rangle\langle E_i^t|$ is the projector onto the eigenstate $|E_i^t\rangle$ of H_t with energy E_i^t, and $U(\tau) \equiv U_t$ is the unitary propagator of the evolution.

Suppose now that our initial system was instead in a non-equilibrium state of the form $\rho^{\mathrm{ne}} = \mathcal{G}_0 + \sum_{i\neq j} \rho_{ij}^{\mathrm{ne}}$. It can be noticed that $p_\tau^{\mathrm{TPM}}(w)$ would remain invariant in this case, since the action of the first projective measurement, performed through Π_n^0, destroys any coherence that could be present in

the initial state. The following question can then be posed: what alternative protocols could be devised such that the initial state coherence would have an effect on the measured thermodynamic work?

Several strategies beyond the TPM scheme have been pointed out in this line [5–7,21–24,32]. Here, we will consider the MH scheme for measuring work, which replaces the first projective measurement of the TPM scheme with a weak measurement [23], and thus allows for initial coherence to survive along the protocol. For an initial state ρ^{ne}, the values of work are now distributed according to

$$p_\tau^{\text{MH}}(w) = \sum_{m,n} P_\tau^{\text{MH}}[E_m^\tau, E_n^0]\delta[w - (E_m^\tau - E_n^0)], \tag{3}$$

where

$$P_\tau^{\text{MH}}[E_m^\tau, E_n^0] = \text{Re}\left(\text{Tr}[U_t^\dagger \Pi_{E_m^\tau} U_t \Pi_{E_n^0} \rho^{\text{ne}}]\right) \tag{4}$$

is the MH quasiprobability distribution, which can take negative values in the range $P_\tau^{\text{MH}}[E_m^\tau, E_n^0] \in [-1/8, 1]$ when the state that we consider deviates from equilibrium [21], and goes back to the distribution associated with a TPM approach for initial equilibrium states.

2.2. Coherence Theory

The coherence of a state can be cast within the framework set by the well-established resource theory of coherence [31,33–36]. As in every quantum resource theory [37], free states and operations must be first identified: here, the set $\mathcal{I}$ of free states—denoted as incoherent states—includes all the states $\delta \in \mathcal{S}(\mathcal{H})$ (with $\mathcal{S}(\mathcal{H})$ denoting the set of unit-trace and semi-positive definite linear operators on $\mathcal{H}$) that are diagonal in some fixed basis $\{|i\rangle\}_{i=0}^{d-1}$ of $\mathcal{H}$, whereas free operations are those that map the set of free states to itself and thus cannot generate coherence. The largest class of free operations are the maximally incoherent operations (MIOs) [33], consisting of all completely positive and trace-preserving (CPTP) maps $\mathcal{M}$ such that $\mathcal{M}(\mathcal{I}) \subset \mathcal{I}$. A subset of MIOs are incoherent operations (IOs) [31], comprising all CPTP maps $\mathcal{M}$ that admit a Kraus representation with operators K_α such that $K_\alpha \mathcal{I} K_\alpha^\dagger \subset \mathcal{I}$ for all α. Only after singling out the states and operations that can be performed at no cost can one investigate how resource states—states with coherence—are to be quantified, manipulated, and interconverted among each other. Coherence measures [31] are indispensable at this stage; quantifying the amount of coherence present in a state $\rho \in \mathcal{S}(\mathcal{H})$, a coherence measure is a functional $C : \mathcal{S}(\mathcal{H}) \to \mathbb{R}_{\geq 0}$ that fulfills the following conditions: (i) faithfulness, meaning that $C(\delta) = 0$ for all $\delta \in \mathcal{I}$, and (ii) monotonicity, $C(\rho) \geq C(\mathcal{M}(\rho))$, for all free operations $\mathcal{M}$.

In particular, throughout this work, we will make use of the l_1-coherence measure [31] defined as

$$C_{l_1}(\rho) = \sum_{i \neq j} |\rho_{ij}|, \tag{5}$$

which is a valid coherence quantifier under IOs, but not MIOs [38]. Notably, when used on qubit states parametrised as $\rho = \frac{1}{2}(\mathbb{1} + \boldsymbol{a} \cdot \boldsymbol{\sigma})$ with $\boldsymbol{a} \in \mathbb{R}^3$, the Bloch vector associated with ρ, and $\boldsymbol{\sigma}$ the vector of Pauli matrices, Equation (5) quantifies the length of the projection $\boldsymbol{a}_\perp$ of $\boldsymbol{a}$ onto the equatorial plane of the Bloch sphere. Thus, for qubit states with $a_z = 0$, we have $a_x = C_{l_1}(\rho)\cos(\chi)$ and $a_y = C_{l_1}(\rho)\sin(\chi)$, where χ is the angle between $\boldsymbol{a}_\perp$ and the x-axis of the Bloch sphere (cf. Figure 1).

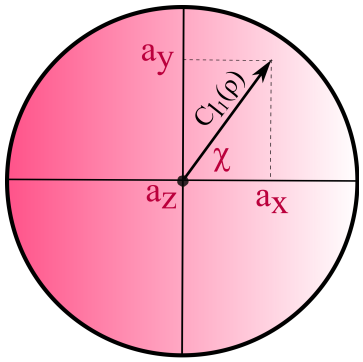

Figure 1. Equatorial plane of the Bloch sphere at $z = 0$. The l_1-coherence of a state quantifies its distance from the z-axis.

3. Main Results

As previously stated, the purpose of this work is to provide a quantitative connection between the TPM scheme and the MH one in terms of quantum coherence. As all the information about a distribution is encoded in its moments, our approach to the assessment of the link between both schemes will rely on quantifying the distance between their corresponding moments.

3.1. Distance between the Averages of Work

The generating function of $p_\tau^{\mathcal{O}}(w)$ is defined as the Fourier transform $G_{\mathcal{O}}(\eta,\tau) = \int dw p_\tau^{\mathcal{O}}(w) e^{i\eta w}$ with $\mathcal{O} = \text{TPM}, \text{MH}$. Moments of work are obtained through differentiation with respect to η, $\langle w_\tau^m \rangle_{\mathcal{O}} = (-i)^k \frac{d^k}{d\eta^k} G_{\mathcal{O}}(\eta,\tau)\big|_{\eta=0}$ [15]. In the TPM scheme, the latter can be written as

$$\langle w_\tau^m \rangle_{\text{TPM}} = \text{Tr}\left[\Delta(\rho_0)(U_\tau^\dagger H_\tau U_\tau - H_0)^m\right], \tag{6}$$

where ρ_0 is the initial state of the working medium and $\Delta(\rho_0) = \sum_n \Pi_n^0 \rho_0 \Pi_n^0$ is the fully dephasing map that suppresses coherences in the energy eigenbasis of the initial Hamiltonian (see notation in Section 2.1). However, the corresponding quantity within the MH approach has the more involved form

$$\langle w_\tau^m \rangle_{\text{MH}} = \frac{1}{2}\sum_{l=0}^{m} \binom{m}{l} \text{Tr}\left[\left\{H_\tau^l, (-H_0)^{m-l}\right\}\rho_0\right], \tag{7}$$

which reduces to $\langle w_\tau^m \rangle_{\text{MH}} = \text{Tr}\left[\rho_0 (U_\tau^\dagger H_\tau U_\tau - H_0)^m\right]$ only for $m = 1, 2$. It then becomes evident that the two first moments of work agree for both distributions whenever $[U_\tau^\dagger H_\tau U_\tau, H_0] = 0$ or $[\rho_0, H_0] = 0$ [32].

If we then consider cyclic processes such that $H_0 = H_\tau \equiv H = \sum_k h_k |k\rangle\langle k|$, we are led to our first result.

Theorem 1. *For a d-dimensional system undergoing a cyclic process described by a unitary evolution U_τ, we have*

$$|\langle w \rangle_{\text{MH}} - \langle w \rangle_{\text{TPM}}| \leq \frac{\text{Tr}|H|}{2} C_{l_1}(\rho_0). \tag{8}$$

The upper bound is tight for qubits, which are such that

$$\max_{U_\tau} |\langle w_\tau \rangle_{\text{MH}} - \langle w_\tau \rangle_{\text{TPM}}| = \frac{\text{Tr}|H|}{2} C_{l_1}(\rho_0), \tag{9}$$

where the maximum is sought over all unitary operations U_τ.

A proof is given in Appendix A. It is worth pointing out that the bound depends on initial time quantities such as $C_{l_1}(\rho_0)$ as well as the Hamiltonian spectrum $\text{Tr}\,[|H|]$, thus clearly highlighting the

role of initial coherences and the impact of the first initial projective measurement on them brought by the TPM scheme.

The tightness of the bound in Equation (8) is quickly lost as the dimension of the information carrier grows. For instance, Figure 2a addresses the case of a system with $d = 3$ showing the values taken by the exact (maximum) difference between the average work corresponding to the two strategies assessed here (red dots)—computed by means of random sampling over the set of initial states ρ—versus the degree of initial coherence in the state of the system. Such quantity is compared to the bound in Equation (8) (blue crosses) to show a widening gap as $C_{l_1}(\rho_0)$ grows. However, a linear-like dependence with respect to the amount of coherence can still be appreciated for the actual maximum distance between average works.

Let us get back to a qubit and consider the case of a sudden Hamiltonian quench, for which $U_\tau \to \mathbb{1}$ in the limit $\tau \to 0$. Under such conditions, we have $\langle w_{\tau\to 0}\rangle_{\mathrm{MH}} = \langle w_{\tau\to 0}\rangle_{\mathrm{TPM}}$, irrespective of the initial coherence. This reflects the fact that both first moments of work will vanish individually under a sudden quench when considering cyclic processes—that is, $\langle w_{\tau\to 0}\rangle_{\mathrm{TPM,MH}} \xrightarrow{U\to\mathbb{1}} 0$.

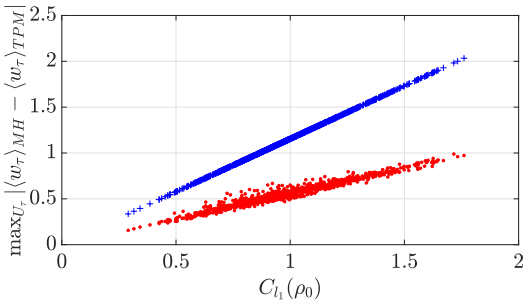

(**a**)

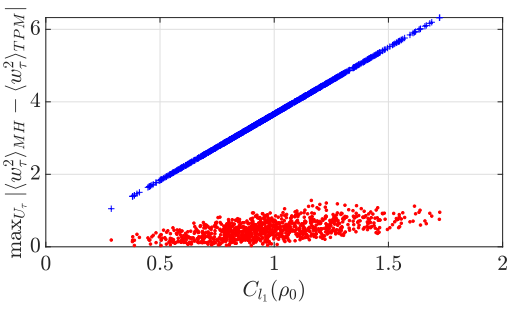

(**b**)

Figure 2. (**a**) Maximum absolute distance between the first moments of work obtained via the Margenau–Hill (MH) scheme and the two-point measurement (TPM) scheme (red dots) and the bound in Equation (8) (blue crosses) versus initial coherence. (**b**) Maximum absolute distance between the second moments of work obtained via the MH scheme and the TPM scheme (red dots) and bound (10) (blue crosses) versus initial coherence. Each point represents a simulation for a different random initial state ρ_0. Both panels refer to a $d = 3$ system governed by the Hamiltonian $H = (1/\sqrt{3})\mathrm{Diag}[1, 1, -2]$.

3.2. Distance between the Variances of Work

The above analysis at the level of the averages of the work distributions is clearly insufficient to satisfactorily characterise the statistical implications of the first projective energy measurement which distinguishes between the TPM and MH schemes. It is in fact well known that measurements induce quantum fluctuations, which become extremely relevant whenever micro- and nano-scale systems are considered. Their connection with thermodynamics has recently drawn much attention and their role as a resource has been clarified [39–41]. Driven by this, we now investigate the relationship between the variances of the work distribution in the TPM and MH schemes. Somehow contrary to intuition,

we will find that a definite general hierarchy between the two cannot be established, i.e., $(\Delta w_\tau)^2_{\mathrm{TPM}}$ is not greater or smaller than $(\Delta w_\tau)^2_{\mathrm{MH}}$ for all parameters. Instead, each particular experimental setup needs to be investigated on its own, as either situation can occur.

Let us first of all focus on the second moment of the work distributions. In the same spirit of Theorem 1, we prove the following:

Theorem 2. *For a d-dimensional system undergoing a cyclic process described by a unitary evolution $U(\tau)$, we have*

$$|\langle w^2_\tau\rangle_{\mathrm{MH}}-\langle w^2_\tau\rangle_{\mathrm{TPM}}|\leq\frac{C_{l_1}}{2}(\rho_0)\left(\mathrm{Tr}H^2+2\max_k|h_k|\mathrm{Tr}|H|\right). \tag{10}$$

A detailed proof is reported in Appendix B. Once again, the bound Equation (10) just depends on initial quantities such as the amount of coherences in the initial state ρ_0 and the energy spectrum of the initial Hamiltonian. It is important to stress that, at variance with the bound in Theorem 1, Equation (10) is not tight, even for qubits. A simple calculation in the case $d = 2$ in fact shows that, while the left hand side is identically zero, i.e., $|\langle w^2\rangle_{\mathrm{MH}} - \langle w^2\rangle_{\mathrm{TPM}}| = 0$, the right hand side does not vanish. In line with the analysis carried out for the discrepancy between first moments, Figure 2b illustrates the diverging gap between the bound in Equation (10) and the maximum difference between second moments for the case of a qutrit ($d = 3$) system with a growing degree of quantum coherence in its initial state.

The difference between variances can be simply calculated as $(\Delta w_\tau)^2_{\mathrm{MH}} - (\Delta w_\tau)^2_{\mathrm{TPM}} = -\langle w_\tau\rangle^2_{\mathrm{MH}} + \langle w_\tau\rangle^2_{\mathrm{TPM}}$. These two considerations allow to show that the above difference does not have a definite sign in general. To show this, let us restrict for simplicity to the case of a qubit undergoing an evolution described by

$$U_\tau = \begin{pmatrix} \cos\tau & \sin\tau \\ -\sin\tau & \cos\tau \end{pmatrix}. \tag{11}$$

Then, it is straightforward to prove the following

Corollary 1. *For a $d = 2$ system undergoing a cyclic process described by a real unitary evolution U_τ, we have*

$$\begin{aligned}(\Delta w_\tau)^2_{\mathrm{MH}} - (\Delta w_\tau)^2_{\mathrm{TPM}} = \\ - f(\rho_0)[f(\rho_0) + 2\sin(\tau)^2 a_z(h_0 - h_1)],\end{aligned} \tag{12}$$

where $f(\rho_0) = (h_0 - h_1)C_{l_1}(\rho_0)\sin(2\tau)\cos(\chi)/2$.

As we see in Figures 3 and 4, the difference between the variances can be either negative or non-negative, so it is not possible to determine which one is larger in general. Restricting to pure real qubits ($a_y = 0 \rightarrow \cos(\chi) = \pm 1$ and $a_z = \pm\sqrt{1 - a_x^2}$) for ease of calculation helps us discern which distribution is more uncertain depending on the values of a_x, as shown in Figure 3 and summarised in Table 1 (further details about the corresponding analysis can be found in Appendix C). The results demonstrate that knowing the value of $C_{l_1}(\rho_0)$ does not suffice to ascertain which variance is larger: rather, it is the sign of $\cos(\chi) = \pm 1$ that eventually dictates their ordering.

Considering the whole set of pure qubits ($a_y \neq 0 \rightarrow \cos(\chi) \neq \pm 1$ and $a_x^2 + a_y^2 + a_z^2 = 1$) would certainly require a much more involved analysis; however, this exceeds the present purposes, which are just to point out that the contribution of $\cos(\chi)$, consistently with what was claimed for real qubits, can never be neglected when assessing the relative uncertainty between distributions (see Figure 4, where the difference between variances is shown to change significantly for different values of χ).

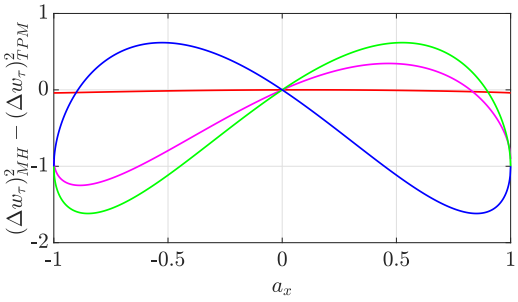

Figure 3. We plot the discrepancy $(\Delta w)^2_{\text{MH}} - (\Delta w)^2_{\text{TPM}}$ between the variances of the TPM and MH distributions for pure states of $d = 2$ systems with Bloch vector $(a_x, 0, \sqrt{1 - a_x^2})$ against a_x. We have taken $H_0 = H_\tau = \sigma_z$ and the dynamics described by Equation (11). We have taken $\tau = 0.1$ (red), $\tau = \pi/5$ (magenta), $\tau = \pi/4$ (green), and $\tau = 3\pi/4$ (blue).

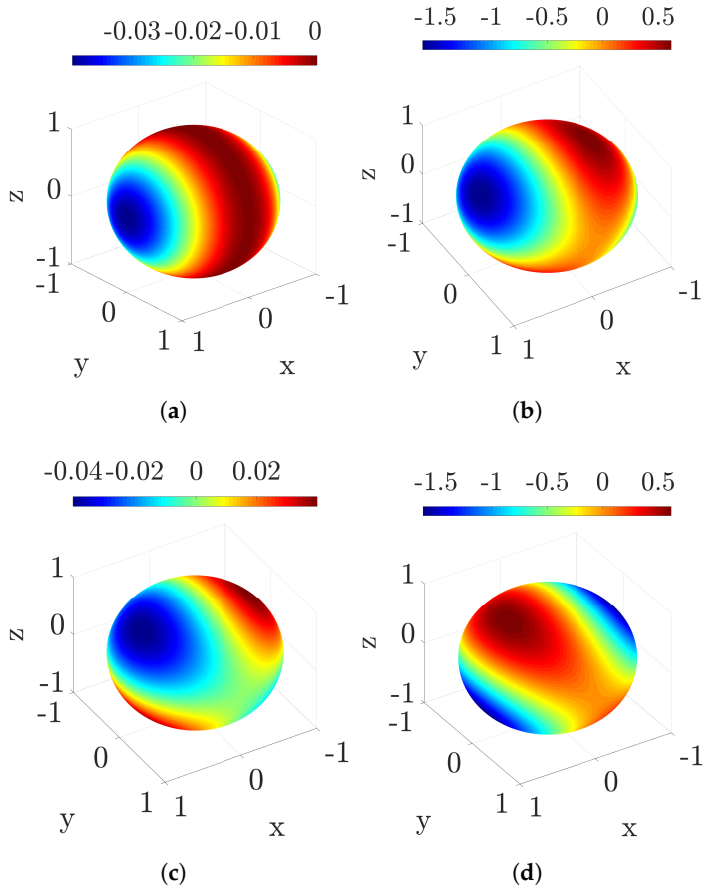

Figure 4. We correlate the value of the discrepancy $(\Delta w_\tau)^2_{\text{MH}} - (\Delta w_\tau)^2_{\text{TPM}}$ between the variances of the TPM and MH distributions to the specific point on the Bloch sphere that represents a pure state of $d = 2$ systems. We have used $H_0 = H_\tau = \sigma_z$, the unitary propagator in Equation (11), and $\tau = 0.1$ (panel (**a**)), $\tau = \pi/4$ (panel (**b**)), $\tau = \pi/2 - 0.01$ (panel (**c**)), and $\tau = 3\pi/4$ (panel (**d**)).

Table 1. Relation between the variances of the MH and the TPM schemes for a two-level system with a Bloch vector with $a_y = 0$ and dynamics ruled by Equation (11). In Table (**a**), we have taken $\mathrm{sgn}(a_z) = \mathrm{sgn}(\tan\tau)$, while Table (**b**) is for $\mathrm{sgn}(a_z) \neq \mathrm{sgn}(\tan\tau)$.

$\mathrm{sgn}(a_z) = \mathrm{sgn}(\tan\tau)$		
$a_x \in [-1, -2a_z \tan\tau]$	$a_x \in [-2a_z \tan\tau, 0]$	$a_x \in [0, 1]$
$(\Delta w)^2_{\mathrm{MH}} \leq (\Delta w)^2_{\mathrm{TPM}}$	$(\Delta w)^2_{\mathrm{MH}} \geq (\Delta w)^2_{\mathrm{TPM}}$	$(\Delta w)^2_{\mathrm{MH}} \leq (\Delta w)^2_{\mathrm{TPM}}$
(**a**)		
$\mathrm{sgn}(a_z) \neq \mathrm{sgn}(\tan\tau)$		
$a_x \in [-1, 0]$	$a_x \in [0, -2a_z \tan\tau]$	$a_x \in [-2a_z \tan\tau, 1]$
$(\Delta w)^2_{\mathrm{MH}} \leq (\Delta w)^2_{\mathrm{TPM}}$	$(\Delta w)^2_{\mathrm{MH}} \geq (\Delta w)^2_{\mathrm{TPM}}$	$(\Delta w)^2_{\mathrm{MH}} \leq (\Delta w)^2_{\mathrm{TPM}}$
(**b**)		

3.3. Study of the Entropy Production

We conclude our analysis by exploiting the above results concerning the work statistics in order to investigate the consequences of initial coherence onto the average entropy production. The latter quantity represents in general a measure of irreversibility and quantifies the amount of work that is dissipated when driving a closed system out of equilibrium. The well-known second law of thermodynamics dictates that the entropy production, defined as the difference between the average work and the free energy difference, is always a non-negative quantity, i.e.,

$$\langle \Sigma_\tau \rangle_{\mathrm{TPM}} \equiv \langle w_\tau \rangle_{\mathrm{TPM}} - \Delta F \geq 0 \tag{13}$$

with $\Delta F_\tau = \beta^{-1} \ln \frac{Z_0}{Z_\tau}$ and $Z_t = \mathrm{Tr}\left[e^{-\beta H_t}\right]$. However, occasional violations to the second law can take place due to the work fluctuations. Remarkably, the above inequality can be turned into an equality; this milestone result, known as the Jarzynski equality [42], states that

$$\langle e^{-\beta(w_\tau - \Delta F_\tau)} \rangle_{\mathrm{TPM}} = 1, \tag{14}$$

from which Equation (13) is recovered by simple application of Jensen's inequality. Crucially, these results rely on the assumption that the system was initially prepared in a thermal state by contact with a bath at inverse temperature β, i.e., $\rho_0 = \mathcal{G}_0 \equiv Z_0^{-1} e^{-\beta \mathcal{H}_0}$. This state, which is clearly incoherent with respect to the initial Hamiltonian, implies that both the TPM and the MH schemes would provide the same answer for the work distribution, as the first energy projective measurement entailed by the TPM approach would not affect the subsequent work statistics. We thus chose for convenience and clarity to use the subscript TPM in order to distinguish from the MH scenario when initial states with finite coherence in the energy eigenbasis are considered.

For an arbitrary initial state ρ_0, however, a modified version of the Jarzynski equality has been shown to hold [21]

$$\langle e^{-\beta(w_\tau - \Delta F_\tau)} \rangle_{\mathrm{MH}} = \mathrm{Re}\left(\mathrm{Tr}[\gamma_\tau \mathcal{G}_0^{-1} \rho_0]\right) \equiv \xi_\tau, \tag{15}$$

where $\gamma_\tau \equiv U_\tau^\dagger \mathcal{G}_\tau U_\tau$. Equation (14) is recovered for $\rho_0 = \mathcal{G}_0$. The consequences of the first projective measurement involved in the TPM scheme, whenever the system possesses initial coherence, can therefore be seen by comparing Equations (15) and (14). In what follows, we will, in particular, complement the analysis carried out in this respect in [21] by studying the average entropy production in the MH scheme, showing that the latter can become negative without being in contradiction with the second law of thermodynamics (which only applies when a TPM scheme is applied).

Thanks to the convexity of the function appearing in Equation (15), one can still apply Jensen's inequality to obtain

$$\langle \Sigma_\tau \rangle_{\mathrm{MH}} = \beta(\langle w_\tau \rangle_{\mathrm{MH}} - \Delta F_\tau) \geq -\ln \xi_\tau, \tag{16}$$

which remarkably does not preclude a negative average entropy production (indeed, $\ln \xi_\tau$ can be arbitrarily large [21]). This happens to hold for small enough β, as we can see in Figure 5a,b, where we have plotted the minimum average entropy production as a function of β, for a suitable qubit evolution, both in the MH and the TPM schemes. From Figure 5b, we also note that both schemes seem to converge for $\beta \to \infty$, which is due to the fact that the coherence of ρ gets smaller as β increases.

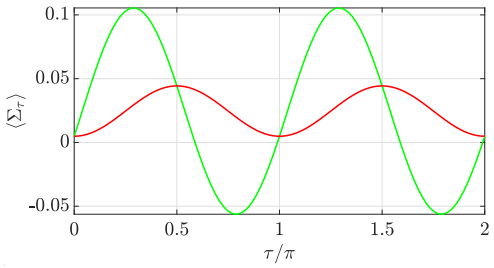

(a)

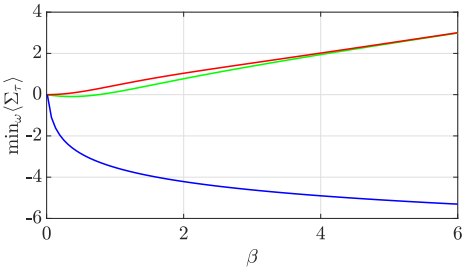

(b)

Figure 5. (**a**) We plot the average entropy production $\langle\Sigma_\tau\rangle$ versus time for $\beta = 0.2$, $\omega = 0.8$. The behavior corresponding to the MH (TPM) scheme is shown by the green (red) curve. (**b**) We show $\min_\omega\langle\Sigma_\tau\rangle$ for the MH and TPM schemes (green and red curves, respectively), and $-\log\xi$ (blue curve) versus β for $\tau = 3\pi/4$.

For both panels, we have taken a qubit prepared in state $\rho = \begin{pmatrix} 1-\alpha^2 & \omega\alpha\sqrt{1-\alpha^2} \\ \omega\alpha\sqrt{1-\alpha^2} & \alpha^2 \end{pmatrix}$ with $\alpha^2 = e^\beta/\mathrm{Tr}[e^{-\beta H_0}]$, $\omega \in [0,1]$ and $H_0 = \sigma_z$, undergoing an evolution given by a real unitary ruled by Equation (11) with $H_\tau = \sigma_z/2$.

In order to get a deeper analytical insight of the regions where $\langle\Sigma_\tau\rangle_{\mathrm{MH}} < 0$, we go to the linear response regime [43]. Here, we prove the following:

Theorem 3. *In the MH scheme, the average entropy production in the linear response regime amounts to*

$$\begin{aligned}\langle\Sigma_\tau\rangle^{\mathrm{LR}}_{\mathrm{MH}} = \beta\langle w_\tau\rangle_{\mathrm{MH}} - \frac{\beta^2}{2}\mathrm{Re}\left\{\mathrm{Tr}\left(\rho_0[H_0, U_\tau^\dagger H_\tau U_\tau]\right)\right\} \\ - \frac{\beta^2}{4}\mathrm{Tr}[H_0^2 - H_\tau^2].\end{aligned} \tag{17}$$

For two-dimensional systems undergoing a process described by a real unitary evolution, $H_0 = \sigma_z$ and $H_\tau = k\sigma_z$ ($k \in \mathbb{R}$), this yields

$$\langle\Sigma_\tau\rangle^{\mathrm{LR}}_{\mathrm{MH}} - \langle\Sigma_\tau\rangle^{\mathrm{LR}}_{\mathrm{TPM}} = \beta k \sin(2\tau)\cos(\chi)C_{l_1}(\rho_0), \tag{18}$$

where $\langle\Sigma_\tau\rangle^{\mathrm{LR}}_{\mathrm{TPM}} = \beta^2(\Delta w_\tau)^2_{\mathrm{TPM}}/2$.

From Equation (18), we see again that both approaches are only equivalent when the initial state is in equilibrium (meaning that $C_{l_1}(\rho_0) = 0$). Moreover, we notice that considering a cyclic process ($k = 1$)

would allow us to recover the relation between the first moments of work obtained in Theorem 1. Finally, we observe that, under a sudden quench, both approaches agree irrespective of the initial state. This must be the case, since it has to be ensured that for $k = 1$ (cyclic processes), both first moments of work vanish under a sudden quench, as argued in Section 3.1,

$$\langle \Sigma_\tau \rangle = \beta \langle w_\tau \rangle = \beta \mathrm{Tr}\rho(U_\tau^\dagger H U_\tau - H) \xrightarrow{U \to \mathbb{1}} 0. \tag{19}$$

We are now equipped to prove the achievability of $\langle \Sigma_\tau \rangle_{\mathrm{MH}} < 0$.

Corollary 2. *In the MH scheme, the average entropy production can take negative values, in contrast to what happens in the TPM scheme:*

$$\langle \Sigma_\tau \rangle_{\mathrm{MH}} \in \mathbb{R}, \text{ whereas } \langle \Sigma_\tau \rangle_{\mathrm{TPM}} \in \mathbb{R}^+ \cup \{0\}. \tag{20}$$

Let us mention that Corollary 2 is independent of the fact that the MH distribution may present negativities. What is more, the ordering of the variances of work obtained in both schemes (see Table 1) cannot explain this result either (more details on these facts can be found in Appendix F).

4. Conclusions

Throughout this work, we have studied the TPM and the MH distributions of work from a systematic comparative approach, being able to assess the difference between both of them in terms of quantum coherence. In particular, we have shown that the difference between the first and second moments of work obtained in both schemes is upper-bounded by the initial coherence, as quantified by the l_1-coherence measure. Regarding the variances of work, we have proved that it is not possible to establish which one is larger in general, since their difference is fundamentally sensitive to the specific configuration of the experiment. Moreover, when restricting to a specific qubit setting, the difference between variances can again be cast via the l_1-coherence of the initial state. This holds as well for the average entropy production, which, in addition, can take negative values, contrary to what is prescribed in the TPM framework.

Our work sheds light on the formal connection between the theory of quantum coherence and recent attempts at going beyond the limitation of the TPM to unveil the statistics of energy fluctuations resulting from quantum processes. Such connection, which is becoming increasingly apparent in light of recent work [3,4,7,8], is likely to embody the *leit motif* of future endeavours aimed at pinpointing the potential advantages of quantum (thermo-)devices.

Author Contributions: All the authors contributed equally to this work. All authors have read and agreed to the published version of the manuscript.

Funding: MGD acknowledges support from Spanish MINECO reference FIS2016-80681-P (with the support of AEI/FEDER,EU) and the Generalitat de Catalunya, project CIRIT 2017-SGR-1127. GG acknowledges support from the European Research Council Starting Grant ODYSSEY (grant nr. 758403). MP acknowledges support from the H2020-FETOPEN-2018-2020 project TEQ (grant nr. 766900), the DfE-SFI Investigator Programme (grant 15/IA/2864), COST Action CA15220, the Royal Society Wolfson Research Fellowship (RSWF\R3\183013), the Royal Society International Exchanges Programme (IEC\R2\192220), the Leverhulme Trust Research Project Grant (grant nr. RGP-2018-266), and the UK EPSRC.

Acknowledgments: MP is grateful to Alessio Belenchia, Stefano Gherardini, Gabriel Landi, and Andrea Trombettoni for fruitful discussions and thanks Mark Mitchison and the organisers of the *"Quarantine Thermo"* seminars series for giving him the opportunity to present some of the results reported here.

Conflicts of Interest: The authors declare no conflict of interest.

Appendix A. Proof of Theorem 1

Here, we provide details on the steps to go through in order to prove the statement made in Theorem 1. We provide such details by addressing Equations (8) and (9) independently.

- **Equation (8)**: The parameterisation of qudit states and unitaries makes finding an exact expression for the absolute difference between average works a difficult task to tackle. However, one can still find an upper bound to such difference as follows:

$$\begin{aligned} |\langle w_\tau\rangle_{\mathrm{MH}} - \langle w_\tau\rangle_{\mathrm{TPM}}| &= \left|\sum_{i\neq j}\rho_{ij}\langle j|U_\tau^\dagger\sum_k h_k|k\rangle\langle k|U_\tau|i\rangle\right| \\ &\leq \sum_{i\neq j}|\rho_{ij}|\sum_k |h_k||\langle j|U_\tau^\dagger|k\rangle\langle k|U_\tau|i\rangle| \\ &\leq \frac{1}{2}\sum_{i\neq j}|\rho_{ij}|\sum_k|h_k| = \frac{1}{2}\mathrm{Tr}|H|C_{l_1}(\rho_0), \end{aligned} \tag{A1}$$

  where we have used the triangle inequality and the fact that the coherence of the pure state $U_\tau^\dagger|k\rangle\langle k|U_\tau$ can never be larger than $1/2$ to achieve the final upper bound.
- **Equation (9)**: When restricting our attention to qubits, we can parameterise unitary operations as $U_\tau = e^{i\frac{\varphi}{2}}\begin{pmatrix} e^{i\varphi_1}\cos\tau & e^{i\varphi_2}\sin\tau \\ -e^{-i\varphi_2}\sin\tau & e^{-i\varphi_1}\cos\tau\end{pmatrix}$, which generalises Equation (11). This gives us

$$\begin{aligned} &|\langle w_\tau\rangle_{\mathrm{MH}} - \langle w_\tau\rangle_{\mathrm{TPM}}| = \\ &= \left|\sum_{i\neq j}\rho_{ij}\langle j|U_\tau^\dagger\sum_k h_k|k\rangle\langle k|U_\tau|i\rangle\right| = \left|\sum_{i\neq j}\rho_{ij}\sum_{k=0,1}h_k\gamma_{ji}^{(k)}\right| = \left|\sum_{i\neq j}\rho_{ij}\left(h_0\gamma_{ji}^{(0)} - h_1\gamma_{ji}^{(0)}\right)\right| \\ &= |h_0-h_1|\left|\rho_{01}\gamma_{10}^{(0)} + \rho_{10}\gamma_{01}^{(0)}\right| = \frac{|h_0-h_1|}{2}\left|\sin(2\tau)\sqrt{a_x^2+a_y^2}\cos\left(\arctan\frac{a_y}{a_x}+\varphi_2-\varphi_1\right)\right| \\ &= \frac{|h_0-h_1|}{2}|\sin(2\tau)||\cos(\chi+\varphi_2-\varphi_1)|\,C_{l_1}(\rho_0) = \frac{\mathrm{Tr}|H|}{2}|\sin(2\tau)|C_{l_1}(\rho_0)|\cos(\chi+\varphi_2-\varphi_1)|, \end{aligned} \tag{A2}$$

  where $\gamma^{(k)} := U_\tau^\dagger|k\rangle\langle k|U_\tau$ and we have used that, for qubit unitaries, $\gamma_{ji}^{(1)} = -\gamma_{ji}^{(0)}$. For a fixed Hamiltonian H, such difference is maximised by choosing $\varphi_2-\varphi_1 = -\chi$ and $\tau = \pi/4$.

Appendix B. Proof of Theorem 2

We now pass to the proof of the statement in Theorem 2, for which we need to go through the following steps.

- **Equation (10)**: By using the triangle inequality, the definition of $\gamma^{(k)}$ given above and the fact that $\gamma_{ji}^{(k)} \leq 1/2$, we can also provide the following upper bound

$$\begin{aligned} |\langle w_\tau^2\rangle_{\mathrm{MH}} - \langle w_\tau^2\rangle_{\mathrm{TPM}}| &\leq \sum_{i\neq j}|\rho_{ij}|\sum_k|h_k^2||\gamma_{ji}^{(k)}| + \sum_{i\neq j}|\rho_{ij}|\sum_l|h_l||h_i||\gamma_{ji}^{(l)}| + \sum_{i\neq j}|\rho_{ij}|\sum_m|h_j||h_m||\gamma_{ji}^{(m)}| \\ &\leq \frac{1}{2}C_{l_1}(\rho_0)\mathrm{Tr}H^2 + \frac{1}{2}C_{l_1}(\rho_0)\max_k|h_k|\mathrm{Tr}|H| + \frac{1}{2}C_{l_1}(\rho_0)\max_k|h_k|\mathrm{Tr}|H|. \end{aligned} \tag{A3}$$

- When focusing on qubits, we have

$$\begin{aligned}
|\langle w_\tau^2\rangle_{\mathrm{MH}} - \langle w_\tau^2\rangle_{\mathrm{TPM}}| &= \left|\sum_{i\neq j}\rho_{ij}\langle j|U_\tau^\dagger H^2 U_\tau - U_\tau^\dagger H U_\tau H - H U_\tau^\dagger H U_\tau|i\rangle\right| \\
&= \left|\sum_{i\neq j}\rho_{ij}\left(\sum_k h_k^2\gamma_{ji}^{(k)} - \sum_l h_l h_i \gamma_{ji}^{(l)} - \sum_m h_j h_m \gamma_{ji}^{(m)}\right)\right| \\
&= \left|\sum_{i\neq j}\rho_{ij}\left[\gamma_{ji}^{(0)}(h_0^2 - h_0 h_i - h_j h_0) + \gamma_{ji}^{(1)}(h_1^2 - h_1 h_i - h_j h_1)\right]\right| \\
&= \left|\sum_{i\neq j}\rho_{ij}\gamma_{ji}^{(0)}\left(h_0^2 - h_0 h_i - h_j h_0 - h_1^2 + h_1 h_i + h_j h_1\right)\right| \\
&= \left|(\rho_{01}\gamma_{10}^{(0)} + \rho_{10}\gamma_{01}^{(0)})(h_0^2 - h_0^2 - h_1 h_0 - h_1^2 + h_1 h_0 + h_1^2)\right| = 0.
\end{aligned} \tag{A4}$$

Appendix C. Derivation of Table 1

We now give an assessment of the relations reported in Table 1. The first thing to notice is that $(\Delta w_\tau)^2_{\mathrm{MH}} - (\Delta w_\tau)^2_{\mathrm{TPM}}$ has roots at $a_x = 0$ and $a_x = -2a_z\tan\tau$, which means that there are two points at which the variances coincide. The first one comes from the equivalence between both schemes when we consider vanishing initial coherence. Moreover, for $a_x = \pm 1$, we have $(\Delta w_\tau)^2_{\mathrm{MH}} - (\Delta w_\tau)^2_{\mathrm{TPM}} = -(h_0 - h_1)^2\cos(\tau)^2\sin(\tau)^2 < 0$. Let us now consider $a_z > 0$ and $\tan\tau > 0$. First, due to Bolzano's theorem, the difference between variances for $a_x \in [-1, -2a_z\tan\tau]$ has to be negative; as it is already negative at $a_x = -1$, having a positive difference within such interval would mean that there should be another root inside it, which is not the case. Second, for the same reason, the difference between variances should have a fixed sign for $a_x \in [-2a_z\tan\tau, 0]$. In particular, such difference must be positive as

$$\left.\frac{\partial[(\Delta w_\tau)^2_{\mathrm{MH}} - (\Delta w_\tau)^2_{\mathrm{TPM}}]}{\partial a_x}\right|_{a_x=-2a_z\tan\tau} = 2(h_0 - h_1)^2 a_z \sin(\tau)^4\left(\frac{1}{\tan\tau} + 4\tan\tau\right) > 0. \tag{A5}$$

Finally, we have that the difference between variances is negative for $a_x \in [0, 1]$, again due to Bolzano's theorem. The same arguments can be applied to the rest of the cases, i.e., $\mathrm{sgn}(a_z) = \mathrm{sgn}(\tan\tau)$ and $\mathrm{sgn}(a_z) \neq \mathrm{sgn}(\tan\tau)$.

Appendix D. Proof of Theorem 3

Let us now move to the proof of Theorem 3.

- **Equation (17)**: The Jarzynski equality [42] $\langle e^{-\beta(w_\tau - \Delta F_\tau)}\rangle_{\mathrm{TPM}} = 1$ is only fulfilled when the initial state is at equilibrium. For an arbitrary initial state ρ, the following fluctuation Theorem applies [21]

$$\langle e^{-\beta(w_\tau - \Delta F_\tau)}\rangle_{\mathrm{MH}} = \mathrm{Re}\left(\mathrm{Tr}[\gamma_\tau \mathcal{G}_0^{-1}\rho_0]\right) \equiv \xi_\tau, \tag{A6}$$

where $\mathcal{G}_\lambda = \dfrac{e^{-\beta H_\lambda}}{\mathrm{Tr}[e^{-\beta H_\lambda}]}$ is a Gibbs state and $\gamma_\tau = U_\tau^\dagger \mathcal{G}_\tau U_\tau$. From here, we get that the free energy difference in the MH scheme is given by

$$\Delta F_\tau = -(\ln\langle e^{-\beta w_\tau}\rangle_{\mathrm{MH}} - \ln\xi_\tau)/\beta. \tag{A7}$$

We use this result in the definition of entropy production $\Sigma = \beta(w - \Delta F)$ and use a cumulant expansion of $\langle e^{-\beta w_\tau}\rangle_{\mathrm{MH}}$ to find [44]

$$\langle \Sigma_\tau \rangle_{\mathrm{MH}} = \sum_{n\geq 2} \frac{(-1)^n}{n!} \kappa_\tau^{(n)}(\beta)\beta^n - \ln \xi_\tau, \tag{A8}$$

where $\kappa_\tau^{(n)}$ are the cumulants of the MH work distribution. Note that we do not take the average of $\ln \xi_\tau$, as it does not contain any stochastic variable w_τ.

In the linear response regime, the first term yields $\frac{\beta^2}{2}(\Delta w_\tau)^2_{\mathrm{MH}}$ [44], where $(\Delta w_\tau)^2_{\mathrm{MH}} = \kappa_\tau^{(2)}(\beta)$ is the variance of the MH distribution of work. Expanding the second term gives

$$\ln \xi_\tau \approx \frac{\beta^2}{4}\mathrm{Tr}[H_0^2 - H_\tau^2] - \beta\langle w_\tau\rangle_{\mathrm{MH}} + \frac{\beta^2}{2}\left\{(\Delta w_\tau)^2_{\mathrm{MH}} + \mathrm{Re}\left(\mathrm{Tr}[\rho_0[H_0, U_\tau^\dagger H_\tau U_\tau]]\right)\right\}. \tag{A9}$$

Thus, the average entropy production in the linear response regime amounts to

$$\langle \Sigma_\tau \rangle^{\mathrm{LR}}_{\mathrm{MH}} = \beta\langle w_\tau\rangle_{\mathrm{MH}} - \frac{\beta^2}{2}\mathrm{Re}\left(\mathrm{Tr}[\rho_0[H_0, U_\tau^\dagger H_\tau U_\tau]]\right) - \frac{\beta^2}{4}\mathrm{Tr}[H_0^2 - H_\tau^2]. \tag{A10}$$

- **Equation (18)**: Let us now have a close look at qubits. For convenience, we consider a qubit prepared in the state $\rho = \frac{1}{2}\begin{pmatrix} 1-a_z & a_x - ia_y \\ a_x + ia_y & 1+a_z \end{pmatrix}$, with $\boldsymbol{a} \in \mathbb{R}^3$, $\frac{1-a_z}{2} = \frac{e^{-\beta}}{\mathrm{Tr}[e^{-\beta H_0}]}$ and $H_0 = \sigma_z$. This ensures that, for small enough β, a_z will also be small:

$$\frac{1-a_z}{2} \approx \frac{1-\beta}{2} \to a_z \approx \beta. \tag{A11}$$

Let us suppose the qubit is subjected to a real unitary transformation U_τ such that $H_\tau = k\sigma_z$, for $k \in \mathbb{C}$. The average entropy production in the linear response regime is then given by Equation (17)

$$\begin{aligned}\langle \Sigma_\tau \rangle^{\mathrm{LR}}_{\mathrm{MH}} &= a_x\beta k \sin(2\tau) - 2a_z\beta k\cos(\tau)^2 + \frac{\beta^2k^2}{2} + a_z\beta k - \frac{\beta^2}{2} + a_z\beta \\ &\approx \beta k \sin(2\tau)\cos(\chi)C_{l_1}(\rho_0) - 2\beta^2 k\cos(\tau)^2 + \frac{\beta^2k^2}{2} + \beta^2 k - \frac{\beta^2}{2} + \beta^2 \\ &= \beta k \sin(2\tau)\cos(\chi)C_{l_1}(\rho_0) - 2\beta^2 k\cos(\tau)^2 + \frac{\beta^2k^2}{2} + \beta^2 k + \frac{\beta^2}{2},\end{aligned} \tag{A12}$$

where we have used that, for small β, $a_z \approx \beta$. As shown in [44], the TPM average entropy production in the linear response regime, where the initial state is set to be in equilibrium, is given by $\langle \Sigma_\tau \rangle^{\mathrm{LR}}_{\mathrm{TPM}} = \frac{\beta^2}{2}(\Delta w_\tau)^2_{\mathrm{TPM}}$. Let us compute it for our qubit evolution

$$\begin{aligned}\langle \Sigma_\tau \rangle^{\mathrm{LR}}_{\mathrm{TPM}} &= 2\beta^2 k(1-\cos(\tau)^2) - 2a_z^2\beta^2k^2\sin(\tau)^4 + 2a_z^2\beta^2k^2\sin(\tau)^2 \\ &\quad - 2a_z^2\beta^2 k\sin(\tau)^2 - \frac{a_z^2\beta^2k^2}{2} + \frac{\beta^2k^2}{2} + a_z^2\beta^2 k - \beta^2 k - \frac{a_z^2\beta^2}{2} + \frac{\beta^2}{2} \\ &\approx -2\beta^2 k\cos(\tau)^2 + \frac{\beta^2k^2}{2} + \beta^2 k + \frac{\beta^2}{2},\end{aligned} \tag{A13}$$

where we have neglected the terms in $a_z^2\beta^2 \approx \beta^4$. Therefore,

$$\langle \Sigma_\tau \rangle^{\mathrm{LR}}_{\mathrm{MH}} = \beta k \sin(2\tau)\cos(\chi)C_{l_1}(\rho_0) + \langle \Sigma_\tau \rangle^{\mathrm{LR}}_{\mathrm{TPM}}. \tag{A14}$$

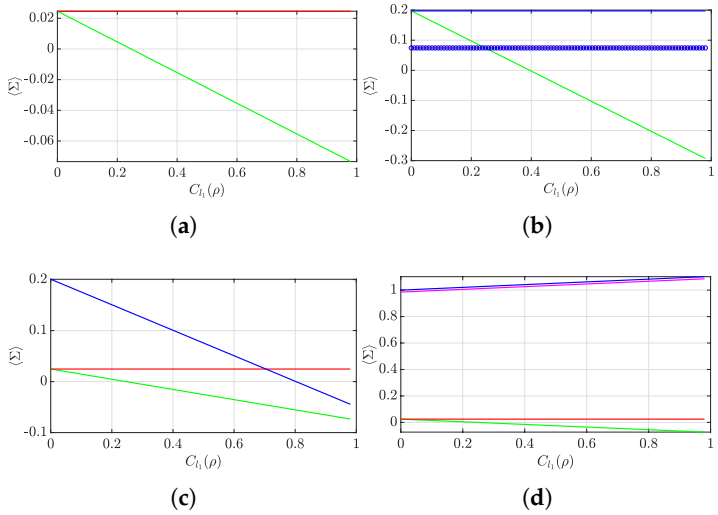

Figure A1. Qubit in the initial state where $\alpha^2 = \frac{e^{\beta}}{\mathrm{Tr}e^{-\beta H(\lambda_0)}}$, $0 \leq \omega \leq 1$ and $H(\lambda_0) = \sigma_z$, undergoing an evolution given by a real unitary $U_\tau = \begin{pmatrix} \cos(\tau) & \sin(\tau) \\ -\sin(\tau) & \cos(\tau) \end{pmatrix}$ and $H(\lambda_\tau) = \frac{1}{2}\sigma_z$. (**a**) $\langle \Sigma_\tau \rangle$ versus initial coherence, $\beta = 0.2$, $\tau = \frac{3\pi}{4}$. MH scheme (green) and TPM scheme (red). (**b**) $\langle w_\tau \rangle_{\mathrm{MH}}$ (green), $\langle w_\tau \rangle_{\mathrm{TPM}}$ (blue line), $\Delta F_{\tau,\mathrm{MH}}$ (red), and $\Delta F_{\tau,\mathrm{TPM}}$ (blue circles) (naturally, they both agree), versus initial coherence, $\beta = 0.2$, $\tau = \frac{3\pi}{4}$. (**c**) $\langle \Sigma_\tau \rangle$ versus initial coherence, $\beta = 0.2$, $\tau = \frac{3\pi}{4}$. MH scheme (green) and TPM scheme (red). Negativity of the MH distribution, computed as $\min_{mn} \mathrm{ReTr}(U_\tau^\dagger |n\rangle\langle n| U_\tau |m\rangle\langle m| \rho_0)$ (blue). (**d**) $\langle \Sigma_\tau \rangle$ versus initial coherence, $\beta = 0.2$, $\tau = \frac{3\pi}{4}$. MH scheme (green) and TPM scheme (red). $\langle e^{-\beta w_\tau} \rangle_{\mathrm{MH}}$ (magenta) and ξ_τ (blue).

Appendix E. Proof of Corollary 2

Consider the qubit case for which Equation (18) holds. For $k = \frac{1}{2}$, $\tau = \frac{3\pi}{4}$ and $\chi = 0$, we have that

$$\langle \Sigma_\tau \rangle_{\mathrm{MH}}^{\mathrm{LR}} = -\frac{\beta}{2} C_{l_1}(\rho_0) + \frac{5\beta^2}{8}, \tag{A15}$$

which becomes negative for $C_{l_1}(\rho_0) > \frac{5\beta}{4}$. For example, for $\beta = 0.2$, the average entropy production is negative when $C_{l_1}(\rho_0) > 0.25$, as it is shown in Figure A1a.

Appendix F. Why Can $\langle \Sigma_\tau \rangle_{\mathrm{MH}}$ Be Negative?

Let us look closely into the case where $\beta \to 0$. In Figure A1a, we can see how the average entropy production changes with the initial coherence. As expected, in the TPM scheme, the entropy remains constant, while in the MH scheme, it decreases, being even able to take negative values. The same can be noticed in Figure 5a. Indeed, for small enough β, the average work calculated in the MH framework can be smaller than the free energy, and even negative (cf. Figure A1b). This immediately suggests why the average entropy production can be negative in the MH scheme: while ΔF_τ is not sensitive to coherence and thus remains constant, $\langle w_\tau \rangle_{\mathrm{MH}}$ keeps on decreasing as the initial coherences increase.

What is more, this fact does not seem to be due to the MH presenting negativities: in Figure A1c, we see that the violation may persist under a non-negative MH distribution. Non-negativities still allow for well-defined logarithms $\ln \langle e^{-\beta w_\tau} \rangle_{\mathrm{MH}}$ and $\ln \xi_\tau$, since $\langle e^{-\beta w_\tau} \rangle_{\mathrm{MH}}$ and ξ_τ are positive, respectively (see Figure A1d). Moreover, the ordering between the variances of work obtained in the MH and the TPM schemes does not seem to provide an explanation on why the average entropy production can be negative in the MH scheme; according to Table 1, the higher uncertainty of the MH scheme compared to that of the TPM scheme ($(\Delta w_\tau)^2_{\mathrm{MH}} \geq (\Delta w_\tau)^2_{\mathrm{TPM}}$) would occur within the interval $0 \leq C_{l_1}(\rho_0) \leq 0.4$. However, the average entropy production in that interval can take any sign. Furthermore, $(\Delta w_\tau)^2_{\mathrm{MH}} \leq$

$(\Delta w_\tau)^2_{\mathrm{TPM}}$ holds for $0.4 \leq C_{l_1}(\rho_0) \leq 1$, where the average entropy production is always negative (see Figure A1a).

References

1. *Thermodynamics in the Quantum Regime*; Binder, F.; Correa, L.; Gogolin, C.; Anders, J.; Adesso, G., Eds.; Springer: Berlin/Heidelberg, Germany, 2019.
2. Deffner, S.; Campbell, S. *Quantum Thermodynamics: An Introduction to the Thermodynamics of Quantum Information*; Morgan & Claypool Publishers: San Rafael, CA, USA, 2019. [CrossRef]
3. Santos, J.P.; Céleri, L.C.; Landi, G.T.; Paternostro, M. The role of quantum coherence in non-equilibrium entropy production. *NPJ Quant. Inf.* **2019**, *5*, 23.
4. Francica, G.; Goold, J.; Plastina. The role of coherence in the non-equilibrium thermodynamics of quantum systems. *Phys. Rev. E* **2019**, *99*, 042105.
5. Riechers, P.M.; Gu, M. Initial-State Dependence of Thermodynamic Dissipation for any Quantum Process. *arXiv* **2020**, arXiv:2002.11425.
6. Sone, A.; Liu, Y.X.; Cappellaro, P. Quantum Jarzynski equality in open quantum systems from the one-time measurement scheme. *arXiv* **2020**, arXiv:2002.06332.
7. Francica, G.; Binder, F.; Guarnieri, G.; Mitchison, M.T.; Goold, J.; Plastina, F. Quantum coherence and ergotropy. *arXiv* **2020**, arXiv:2006.05424. [CrossRef]
8. Francica, G.; Goold, J.; Plastina, F.; Paternostro, M. Daemonic Ergotropy: Enhanced Work Extraction from Quantum Correlations. *NPJ Quant. Inf.* **2017**, *3*, 12. [CrossRef]
9. Bernards, F.; Kleinmann, M.; Gühne, O.; Paternostro, M. Daemonic Ergotropy: Generalised Measurements and Multipartite Settings. *Entropy* **2019**, *21*, 771.
10. Miller, H.J.D.; Mohammady, M.H.; Perarnau-Llobet, M.; Guarnieri, G. Thermodynamic uncertainty relation in slowly driven quantum heat engines. *arXiv* **2020**, arXiv:2006.07316. [CrossRef]
11. Miller, H.J.; Scandi, M.; Anders, J.; Perarnau-Llobet, M. Work Fluctuations in Slow Processes: Quantum Signatures and Optimal Control. *Phys. Rev. Lett.* **2019**, *123*.
12. Scandi, M.; Miller, H.J.D.; Anders, J.; Perarnau-Llobet, M. Quantum work statistics close to equilibrium. *arXiv* **2019**, arXiv:1911.04306. [CrossRef]
13. Talkner, P.; Lutz, E.; Hänggi, P. Fluctuation theorems: Work is not an observable. *Phys. Rev. E* **2007**, *75*, 050102. [CrossRef]
14. Campisi, M.; Hänggi, P.; Talkner, P. Colloquium: Quantum fluctuation relations: Foundations and applications. *Rev. Mod. Phys.* **2011**, *83*, 771. [CrossRef]
15. Esposito, M.; Harbola, U.; Mukamel, S. Nonequilibrium fluctuations, fluctuation theorems, and counting statistics in quantum system. *Rev. Mod. Phys.* **2009**, *81*, 1665. [CrossRef] [PubMed]
16. Batalhão, T.B.; Souza, A.M.; Mazzola, L.; Auccaise, R.; Sarthour, R.S.; Oliveira, I.S.; Goold, J.; De Chiara, G.; Paternostro, M.; Serra, R.M. Experimental reconstruction of work distribution and study of fluctuation relations in a closed quantum system. *Phys. Rev. Lett.* **2014**, *113*, 140601. [CrossRef]
17. An, S.; Zhang, J.N.; Um, M.; Lv, D.; Lu, Y.; Zhang, J.; Yin, Z.Q.; Quan, H.; Kim, K. Experimental test of the quantum Jarzynski equality with a trapped-ion system. *Nat. Phys.* **2015**, *11*, 193–199. [CrossRef] [PubMed]
18. Peterson, J.P.; Batalhão, T.B.; Herrera, M.; Souza, A.M.; Sarthour, R.S.; Oliveira, I.S.; Serra, R.M. Experimental characterization of a spin quantum heat engine. *Phys. Rev. Lett.* **2019**, *123*, 240601. [CrossRef]
19. Ronzani, A.; Karimi, B.; Senior, J.; Chang, Y.C.; Peltonen, J.T.; Chen, C.; Pekola, J.P. Tunable photonic heat transport in a quantum heat valve. *Nat. Phys.* **2018**, *14*, 991–995. [CrossRef]
20. von Lindenfels, D.; Gräb, O.; Schmiegelow, C.T.; Kaushal, V.; Schulz, J.; Mitchison, M.T.; Goold, J.; Schmidt-Kaler, F.; Poschinger, U.G. Spin Heat Engine Coupled to a Harmonic-Oscillator Flywheel. *Phys. Rev. Lett.* **2019**, *123*, 080602. [CrossRef]
21. Allahverdyan, A.E. Nonequilibrium quantum fluctuations of work. *Phys. Rev. E* **2014**, *90*, 032137. [CrossRef]
22. Micadei, K.; Landi, G.T.; Lutz, E. Quantum Fluctuation Theorems beyond Two-Point Measurements. *Phys. Rev. Lett.* **2020**, *124*, 090602.
23. Levy, A.; Lostaglio, M. A quasiprobability distribution for heat fluctuations in the quantum regime. *arXiv* **2019**, arXiv:1909.11116.

24. Gherardini, S.; Belenchia, A.; Paternostro, M.; Trombettoni, A. The role of quantum coherence in energy fluctuations. *arXiv* **2020**, arXiv:2006.06208.
25. Solinas, P.; Gasparinetti, S. Full distribution of work done on a quantum system for arbitrary initial states *Phys. Rev. E* **2015**, *92*, 042150. [CrossRef]
26. de Falco D.; Tamascelli D. Noise-assisted quantum transport and computation. *J. Phys. A Math. Theor. 2013*, *22*, 5301–5316. [CrossRef]
27. Solinas, P.; Gasparinetti, S. Probing quantum interference effects in the work distribution. *Phys. Rev. A* **2016**, *94*, 052103.
28. Terletsky, Y.P. The limiting transition from quantum to classical mechanics. *J. Exp. Theor. Phys.* **1937**, *7*, 1290. [CrossRef]
29. Margenau, H.; Hill, R.N. Correlation between measurements in quantum theory. *Prog. Theor. Phys.* **1961**, *26*, 722. [CrossRef]
30. Kirkwood, J.G. Quantum statistics of almost classical assemblies. *Phys. Rev.* **1933**, *44*, 37. [CrossRef]
31. Baumgratz, T.; Cramer, M.; Plenio, M.B. Quantifying Coherence. *Phys. Rev. Lett.* **2014**, *113*, 140401. [CrossRef]
32. Miller, H.J.D.; Anders, J. Time-reversal symmetric work distributions for closed quantum dynamics in the histories framework. *New J. Phys.* **2017**, *19*, 062001. [CrossRef]
33. Åberg, J. Quantifying Superposition. *arXiv* **2006**, arXiv:0612146. [CrossRef]
34. Braun, D.; Georgeot, B. Quantitative measure of interference. *Phys. Rev. A* **2006**, *73*, 022314. [CrossRef]
35. Streltsov, A.; Adesso, G.; Plenio, M.B. Colloquium: Quantum coherence as a resource. *Rev. Mod. Phys.* **2017**, *89*, 041003. [CrossRef] [PubMed]
36. Winter, A.; Yang, D. Operational Resource Theory of Coherence. *Phys. Rev. Lett.* **2016**, *116*, 120404. [CrossRef] [PubMed]
37. Brandão, F.G.S.L.; Gour, G. Reversible Framework for Quantum Resource Theories. *Phys. Rev. Lett.* **2015**, *115*, 070503.
38. Bu, K.; Xiong, C. A Note on Cohering Power and De-cohering Power. *Quant. Inf. Comput.* **2017**, *17*, 1206–1220. [CrossRef]
39. Ding, X.; Yi, J.; Kim, Y.W.; Talkner, P. Measurement-driven single temperature engine. *Phys. Rev. E* **2018**, *98*, 042122. [CrossRef]
40. Elouard, C.; Herrera-Martí, D.; Huard, B.; Auffèves, A. Extracting Work from Quantum Measurement in Maxwell's Demon Engines. *Phys. Rev. Lett.* **2017**, *118*, 260603. [CrossRef]
41. Buffoni, L.; Solfanelli, A.; Verrucchi, P.; Cuccoli, A.; Campisi, M. Quantum Measurement Cooling. *Phys. Rev. Lett.* **2019**, *122*. [CrossRef]
42. Jarzynski, C. Nonequilibrium equality for free energy differences. *Phys. Rev. Lett.* **1997**, *78*, 2690–2693.
43. Kubo, R. Statistical-mechanical theory of irreversible processes. I. General theory and simple applications to magnetic and conduction problems. *J. Phys. Soc. Jpn.* **1957**, *12*, 570–586. [CrossRef] [PubMed]
44. Batalhão, T.B.; Souza, A.M.; Sarthour, R.S.; Oliveira, I.S.; Paternostro, M.; Lutz, E.; Serra, R.M. Irreversibility and the arrow of time in a quenched quantum system. *Phys. Rev. Lett.* **2015**, *115*, 190601.